INSTITUTE OF PHYSICS PUBLISHING JOURNAL OF PHYSICS: CONDENSED MATTER

J. Phys.: Condens. Matter **18** (2006) 7893–7904 doi:10.1088/0953-8984/18/34/004

A combined study of the magnetic properties of $GdCrO_4$

E Jiménez-Melero[1,7], P C M Gubbens[2], M P Steenvoorden[2], S Sakarya[2], A Goosens[2], P Dalmas de Réotier[3], A Yaouanc[3], J Rodríguez-Carvajal[4], B Beuneu[4], J Isasi[1], R Sáez-Puche[1], U Zimmerman[5] and J L Martínez[6]

[1] Departamento de Química Inorgánica, Fac. C. Químicas, Universidad Complutense de Madrid, 28040-Madrid, Spain
[2] Fundamental Aspects of Materials and Energy, Faculty of Applied Sciences, Delft University of Technology, Mekelweg 15, 2629 JB Delft, The Netherlands
[3] CEA Grenoble, DRFMC/SPSMS, F-38054 Grenoble Cedex 9, France
[4] Laboratoire Leon-Brillouin, (CEA-CNRS) Saclay, Gif sur Yvette Cedex 91191, France
[5] Paul Scherer Institut, 5232 Villigen PSI, Switzerland
[6] Instituto de Ciencia de Materiales de Madrid, Consejo Superior de Investigaciones Científicas, Cantoblanco, 28049-Madrid, Spain

E-mail: E.Melero@tnw.tudelft.nl

Received 20 March 2006, in final form 18 June 2006
Published 7 August 2006

Abstract

We have performed a detailed study of the magnetic properties of $GdCrO_4$ at low temperatures by complementary use of different macroscopic and microscopic physical techniques. A ferromagnetic order is established in this oxide below $T_C = 22$ K. The ordered magnetic moments of the Cr^{5+} ions are located along the crystallographic c-axis, forming an angle of $\approx 24°$ with the ordered moments of the Gd^{3+} ions. Surprisingly, only 20% of the Gd^{3+} sublattice orders at the Curie temperature of 22 K, while the remaining 80% stays paramagnetic down to around 10 K. This 80% of the Gd^{3+} ions may be ascribed to a low-temperature orthorhombic phase. Moreover, the Gd^{3+} magnetic order seems to be triggered by a relatively large transferred hyperfine field coming from the Cr^{5+} sublattice.

(Some figures in this article are in colour only in the electronic version)

1. Introduction

$RCrO_4$ oxides constitute a subgroup of the family of RXO_4 compounds, where R = rare earth ion and X = P, As, Cr, V [1, 2]. The strong interest in the rare earth chromates stems from the presence of two magnetic ions in the structure, namely Cr^{5+} and R^{3+}, and from the high

---

[7] Author to whom any correspondence should be addressed. Present address: Fundamental Aspects of Materials and Energy, Faculty of Applied Sciences, Delft University of Technology, Mekelweg 15, 2629 JB Delft, The Netherlands.

symmetry of the crystal structure at room temperature, where only one crystallographic site is expected for each of the mentioned ions. These two facts make the $RCrO_4$ group of compounds an adequate system for gaining insight into the microscopic nature of the 3d–4f magnetic interactions. Within this framework, $GdCrO_4$ has attracted significant attention due to the lack of intrinsic magnetic anisotropy in the rare earth sublattice. Accordingly, both Cr^{5+} and Gd^{3+} ions behave as magnetically isotropic [3, 4]. Therefore, the effect of the intrinsic magnetic anisotropy of the rare earth sublattice on the overall magnetic properties of the remaining $RCrO_4$ compounds can be adequately evaluated in subsequent studies. In this sense, a magnetic ordering has been previously reported in all members of the $RCrO_4$ family of compounds, the critical temperatures being lower than 30 K in all cases. However, some important questions remain to be answered about their magnetic properties, such as: why does the sign of the predominant magnetic interactions change notably from one compound to another [5]? Or why do the magnetic ordering temperatures not show a deGennes behaviour, as found in other rare earth-containing oxides such as R_2CuBaO_5 [6]?

We have undertaken a thorough study of the magnetic properties of $GdCrO_4$ by complementary use of different physical techniques. Previous x-ray diffraction experiments indicate that this oxide crystallizes at room temperature with a zircon-type structure [2]. Moreover, it presents a ferromagnetic order at temperatures lower than $T_C = 21.7(5)$ K [5]. The performance of neutron diffraction experiments on $GdCrO_4$ has been triggered by the need to obtain further and more accurate information about the crystallographic features of this oxide, as well as for study of the evolution of its crystal structure from room temperature down to 2 K. After the structural characterization, we proceeded to carry out a systematic study of the magnetic properties of $GdCrO_4$, starting with macroscopic measurements such as magnetic susceptibility, magnetization and specific heat. The obtained results have served as an adequate basis for planning the low-temperature neutron diffraction experiments, so as to determine the magnetic structure of $GdCrO_4$. Furthermore, we have employed the ^{155}Gd Mössbauer spectroscopy and muon spin rotation (μSR) techniques to gain valuable local information about its magnetic properties at low temperatures. The experimental results for $YCrO_4$ have proved useful for evaluating the role of the Gd^{3+}–Cr^{5+} interactions in the overall magnetic properties of $GdCrO_4$. Likewise, the influence of the Cr^{5+} ion can be conveniently assessed by taking as a reference the isostructural gadolinium vanadate ($GdVO_4$).

2. Sample preparation and experimental details

The $YCrO_4$ and $GdCrO_4$ samples were prepared by using the nitrate precursor method [7]. Stoichiometric amounts of $R(NO_3)_3{\cdot}6H_2O$ (R = Y and Gd) and $Cr(NO_3)_3{\cdot}9H_2O$ were weighed and mixed together. The resultant mixture was then heated according to the following thermal scheme: 30 min at 433 K, 30 min at 473 K and 24 h at 773 K. A flow of oxygen was required during the synthesis process in order to stabilize the Cr^{5+} ion. Afterwards, the obtained green-coloured powdered samples were characterized by room-temperature x-ray diffraction.

The following temperature-dependent neutron diffraction experiments were performed at the 7C2 diffractometer of the Laboratoire Léon-Brillouin (Saclay, France) with a wavelength of $\lambda = 0.6946$ Å [8]. It is important to highlight here the large absorption cross section of natural gadolinium nuclei for thermal neutrons [9]. This constitutes a serious drawback for the successful performance of neutron diffraction experiments on gadolinium-containing samples. However, the probability for gadolinium nuclei to absorb neutrons reduces significantly when the wavelength is decreased. The choice of wavelength of $\approx$0.7 Å is the result of a compromise between the beam flux (increasing with the wavelength) and the absorption. The sample geometry was chosen to maximize the signal: a double-walled cylinder of diameter

10 mm × 12 mm occupying the whole beam size with a small sample thickness and hence a reduced absorption. We have also measured the empty vanadium sample holder in the same experimental conditions as the $GdCrO_4$ sample, in order to correct the experimental data of the latter for both the background and the weak Bragg reflections coming from the vanadium. Moreover, the neutron diffraction pattern of a standard nickel sample was recorded to accurately determine both the neutron wavelength and the instrumental resolution parameters. The analysis of the diffraction data was based on the Rietveld method implemented in the program Fullprof [10, 11].

Magnetic susceptibility and magnetization measurements were performed in a Quantum Design XL-SQUID magnetometer at different fields in the temperature range of 2–300 K. The experimental data were corrected for the diamagnetic contribution of the constituent ions [12]. The specific heat of $GdCrO_4$ was measured in a Quantum Design PPMS set-up based on the thermal relaxation method [13]. A temperature range of 1.7–300 K was covered during the experiments, both in the absence and in the presence of different applied magnetic fields with a maximum value of $\mu_0 H_{\mathrm{ex}} = 9$ T. A small portion of the sample was initially pressed into a pellet and then sintered at a temperature of 773 K for 12 h. It was then fixed to the sapphire platform of the set-up by Apiezon grease. The specific heat of the grease was measured separately at different temperatures and then subtracted from the experimental values of the specific heat of $GdCrO_4$.

The hyperfine fields (H_{eff}) and the electric quadrupolar splittings (QS $= \frac{1}{2}eQV_{zz}$, with a nuclear quadrupolar moment of $Q = 1.30$ b [14]) of $GdCrO_4$ were measured using the 86.54 keV resonance of ^{155}Gd Mössbauer spectroscopy. The source consisted of neutron irradiated $SmPd_3$, enriched to 98% in ^{154}Sm. Both the source and the absorber were cooled in a helium cryostat, in order to reach significant values of the recoilless fraction. The Doppler velocity of the transducer, working in a constant acceleration mode, was calibrated with the ^{57}Fe Mössbauer spectra of α-Fe_2O_3. Further details of the experimental set-up can be found elsewhere [15]. The $GdCrO_4$ spectra were analysed by means of a least-square fitting procedure involving the diagonalization of the full nuclear Hamiltonian and using a transmission integral.

The μSR technique uses the positive muon as a very sensitive local magnetic probe. The polarized muons are implanted in the sample, where their polarization evolves in the local magnetic field until they decay (the muon lifetime is $\tau_\mu \approx 2.2\ \mu$s). The decay positron is emitted preferentially along the muon spin direction. By collection of several millions of positrons as a function of time, one can reconstruct the time dependence of the spin polarization which, in turn, reflects the distribution of magnetic fields at the muon site. We have collected the muon spectra of both $GdCrO_4$ and $YCrO_4$ samples at different temperatures in the absence of an external magnetic field. More detailed information about the μSR technique can be found in [16, 17]. The μSR measurements were performed at the GPD set-up of the Paul Scherer Institute (PSI) in Switzerland [18].

3. Experimental results and discussion

3.1. Structural characterization

The analysis of the room-temperature x-ray diffraction pattern confirms the zircon-type structure in $GdCrO_4$, and permits us to exclude the presence of any secondary phase [19]. This structural type is characterized by the tetragonal space group $I4_1/amd$. Both the R^{3+} and Cr^{5+} ions occupy special positions, namely 4a $(0, \frac{3}{4}, \frac{1}{8})$ and 4b $(0, \frac{1}{4}, \frac{3}{8})$, respectively, while the oxygen atoms are located in the 16h $(0, y, z)$ positions [2, 20]. The R^{3+} ions are surrounded by eight oxygen atoms forming a polyhedron $[RO_8]$ known as a bisdisphenoid. By

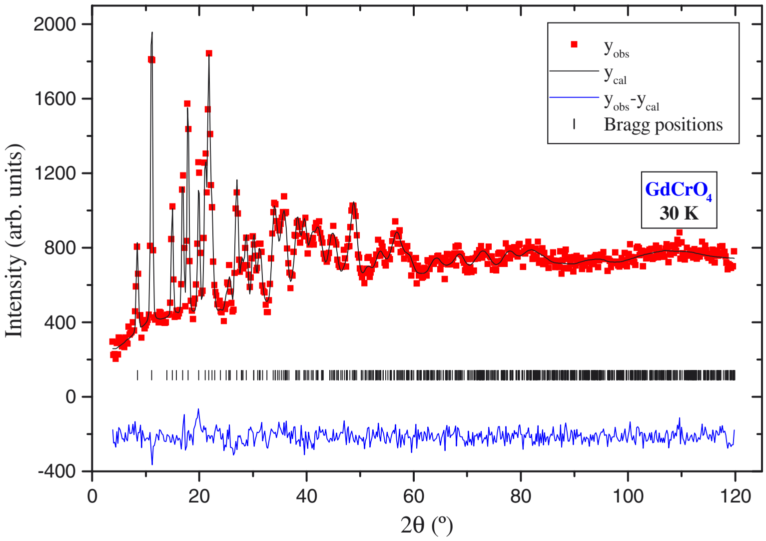

Figure 1. Neutron diffraction pattern of $GdCrO_4$ at 30 K, refined on the basis of the zircon-type structure.

Table 1. Experimental values of the lattice parameters, bond distances and angles, and the reliability factors of the refinements (R_F and R_{wp}) of $GdCrO_4$ at different temperatures.

T (K)	a (Å)	c (Å)	d (Cr–O) (Å)	O–Cr–O (deg)	d (Gd–O) (Å)	O–Gd–O (deg)		R_F	R_{wp}
300	7.170(2)	6.286(2)	1.688(7) × 4	114.4(5) × 2 100.0(4) × 2	2.352(7) × 4 2.432(5) × 4	155.8(5) × 2 136.1(4) × 4	92.5(3) × 4 63.8(2) × 2	4.8	20.0
30	7.173(2)	6.281(2)	1.692(6) × 4	113.9(5) × 2 100.8(6) × 2	2.335(6) × 4 2.441(5) × 4	155.6(5) × 2 135.6(4) × 4	92.5(3) × 4 64.6(2) × 2	3.0	18.9
10	7.172(2)	6.282(2)	1.694(7) × 4	113.9(5) × 2 100.9(6) × 2	2.332(7) × 4 2.441(5) × 4	155.7(6) × 2 135.5(4) × 4	92.6(3) × 4 64.7(2) × 2	2.7	16.1
2	7.166(2)	6.278(2)	1.692(8) × 4	114.2(6) × 2 100.5(7) × 2	2.333(8) × 4 2.433(6) × 4	155.9(6) × 2 135.6(5) × 4	92.5(4) × 4 64.6(2) × 2	3.1	17.8

contrast, the Cr^{5+} ions are located inside oxygen tetrahedra [CrO_4] [21]. The obtained values for the structural parameters of $GdCrO_4$ have been used as initial estimates for the refinement of its neutron diffraction data at different temperatures between 2 and 300 K. Figure 1 shows the refined neutron diffraction pattern of $GdCrO_4$ at 30 K. This oxide retains its tetragonal symmetry from room temperature down to 2 K.

Table 1 collects the experimental values of the structural parameters at several temperatures. The volume of the unit cell decreases from 323.16(1) Å^3 to 322.38(1) Å^3 from room temperature to 2 K, which implies a reduction of ≈0.24%. Moreover, the oxygen atomic coordinates obtained by neutron diffraction present a higher accuracy than those initially derived from x-ray diffraction experiments. This fact is due to the relatively low scattering power of the oxygen atoms for x-rays, as compared to that of the Cr^{5+} and specially the Gd^{3+} ions. At room temperature, the derived oxygen coordinates are (0, 0.429(1), 0.203(1)). Furthermore, the [CrO_4] tetrahedra remain unaltered within the experimental uncertainty when decreasing the temperature. By contrast, one of the experimental Gd–O bond distances suffers a significant reduction.

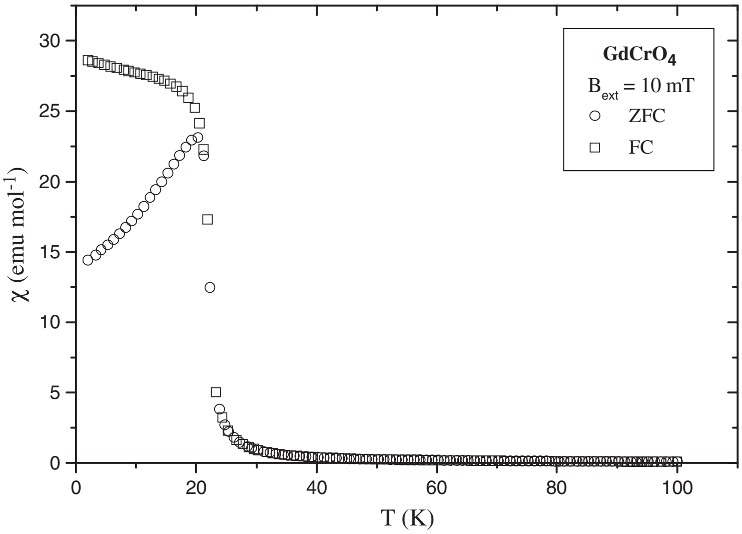

Figure 2. Temperature dependence of the magnetic susceptibility of GdCrO$_4$ between 2 and 100 K in the presence of an applied magnetic field of $\mu_0 H_{\mathrm{ex}} = 10$ mT, during the processes of field-cooling (FC) and field-warming after zero-field cooling (ZFC).

3.2. Bulk magnetic measurements

Figure 2 displays the temperature dependence of the magnetic susceptibility of GdCrO$_4$ between 2 and 100 K in the presence of an applied field of $\mu_0 H_{\mathrm{ex}} = 10$ mT. The measurements were performed for both field-cooling of the sample (FC) and field-warming after a zero-field cooling process (ZFC). The magnetic susceptibility obeys a Curie–Weiss law between room temperature and 30 K, with a value for the Curie–Weiss temperature of $\theta_{\mathrm{CW}} = 21.2(3)$ K. Moreover, at temperatures lower than 22 K, there is a noticeable difference in the experimental values of the magnetic susceptibility between the FC and ZFC processes. Such a difference constitutes a clear indication of the occurrence of a net ferromagnetic component in GdCrO$_4$ below 22 K.

Afterwards, the isothermal magnetization was measured as a function of the external magnetic field, as shown in figure 3. The magnetization curves at 2, 10 and 20 K resemble the behaviour of a ferromagnetic compound. It is important to stress that the magnetization at 2 K and 5 T takes a value larger than 7 μ_{B}. Based on the theoretical value for the ordered magnetic moment of the Gd^{3+} ion ($gJ = 7\ \mu_{\mathrm{B}}$) [4], we can conclude that both Gd^{3+} and Cr^{5+} ions are involved in the magnetic ordering at 2 K.

3.3. Specific heat data

Figure 4 shows the variation of the magnetic contribution to the specific heat of this oxide between 2 and 30 K in the absence of an applied magnetic field, together with the associated variation of entropy, after having subtracted both the lattice and electronic contributions to the specific heat [5, 22]. There is a clear maximum at a temperature of 21.1 K, which corresponds to the Curie temperature previously determined by magnetic susceptibility measurements. However, there is a second weaker anomaly at temperatures lower than 8 K, attaining its maximum value at 4.8 K. The application of an external magnetic field influences significantly both anomalies, and they have almost disappeared at an applied field of $\mu_0 H_{\mathrm{ex}} = 9$ T. This field-dependent effect indicates that both transitions have a magnetic origin.

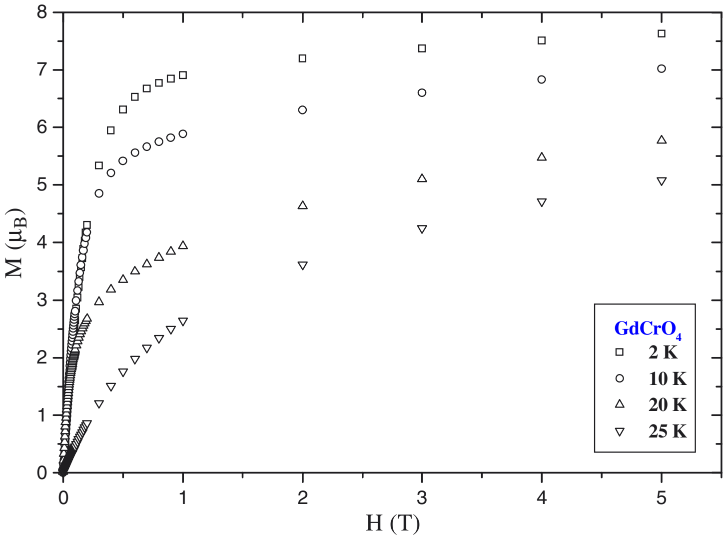

Figure 3. Field-dependent magnetization curves of GdCrO$_4$ at different measurement temperatures.

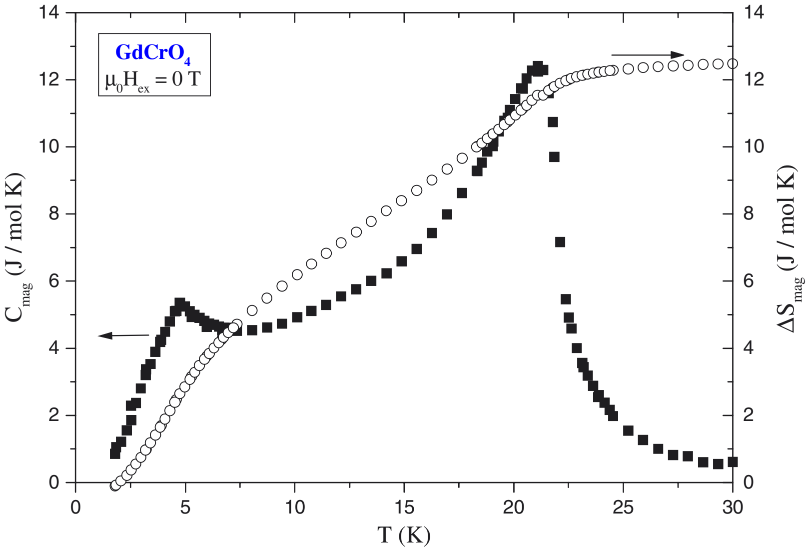

Figure 4. Magnetic contribution to the specific heat of GdCrO$_4$ between 2 and 30 K in the absence of an applied magnetic field, coupled with the associated variation of entropy.

In general, the change in magnetic entropy for an ion with a spin quantum number '*S*' equals [23]:

$$\Delta S_t = R \ln(2S + 1). \tag{1}$$

Therefore, the theoretical values for the Cr^{5+} ($S = 1/2$) and Gd^{3+} ($S = 7/2$) ions are 5.76 and 17.29 J mol^{-1} K^{-1}, respectively. By discounting the theoretical contribution of Cr^{5+} from the experimentally determined change in entropy of GdCrO$_4$ ($\Delta S_t = 12.48$ J mol^{-1} K^{-1}), we arrive at a value of 6.72 J mol^{-1} K^{-1} for the magnetic contribution of Gd^{3+}. This latter

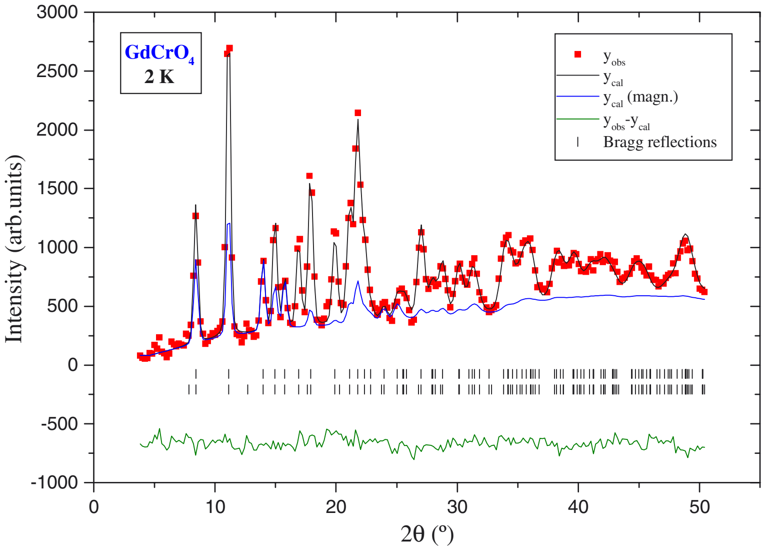

Figure 5. Neutron diffraction pattern of $GdCrO_4$ at 2 K, refined on the basis of the zircon-type structure and the proposed magnetic structure (see text). The term y_{cal} (magn.) denotes the magnetic contribution to the neutron diffraction pattern of $GdCrO_4$.

value is significantly reduced in comparison to the theoretical one. The discrepancy may be attributed to an intense internal magnetic field, that would be causing a large Zeeman splitting of the $S = 7/2$ ground state of the Gd^{3+} ion. As a consequence, only some of the Gd^{3+} Zeeman-split energy levels will be involved in the magnetic transitions observed in $GdCrO_4$ at low temperatures. Since the isostructural $GdVO_4$ compound presents an antiferromagnetic order below 2.495 K [24, 25], such an internal magnetic field cannot be properly ascribed to the Gd–Gd magnetic interactions. Accordingly, the Gd–Cr magnetic interactions are quite intense in $GdCrO_4$.

3.4. Magnetic structure determination

Determination of the magnetic structure of $GdCrO_4$ has been performed by analysing its neutron diffraction patterns at 30, 10 and 2 K. There is an almost complete coincidence between the experimental data obtained at different temperatures between 30 and 300 K, with only subtle changes in the tetragonal crystal structure of this compound (see section 3.1). However, at lower temperatures the intensity of certain reflections increases with decreasing temperature. This indicates the contribution of a magnetic component on top of nuclear Bragg reflections. Moreover, we can also observe the appearance of two additional Bragg reflections at a scattering angle of $\approx 14°$ and 15.8°, whose nuclear contribution seems to be negligible. Figure 5 displays the refined neutron diffraction pattern of $GdCrO_4$ at 2 K. The mentioned experimental magnetic contribution can be indexed successfully on the basis of the propagation vector $\mathbf{k} = (000)$. The best agreement between the experimental and calculated neutron diffraction patterns has been obtained with a ferromagnetic coupling of the ordered magnetic moments of the Cr^{5+} sublattice along the crystallographic c-axis. The main component of the Gd^{3+} magnetization is also placed in the c-axis. However, there seems to be an additional smaller ferromagnetic component of the Gd^{3+} ions situated in the basal plane of the crystal structure. At the lowest measuring temperature of 2 K, the ordered moment of the Cr^{5+} ion

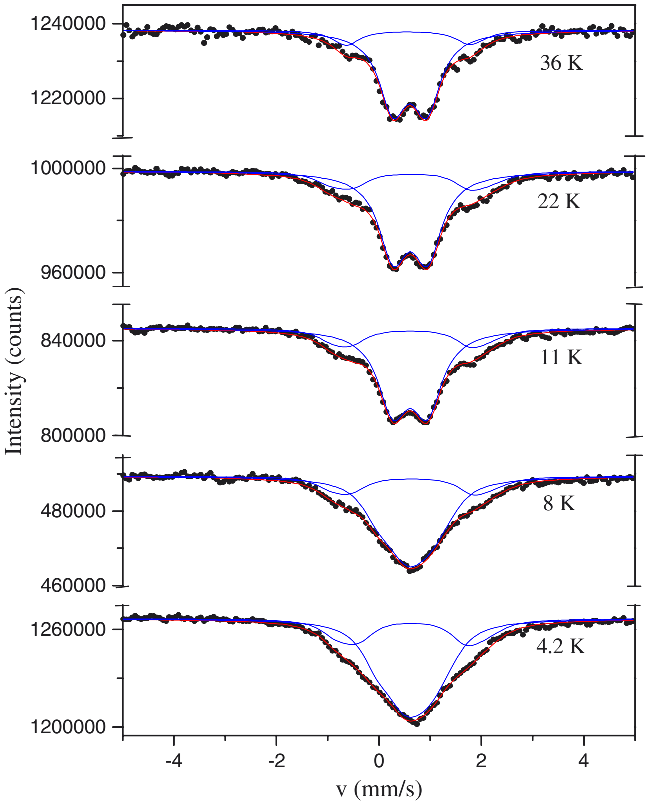

Figure 6. ^{155}Gd Mössbauer spectra of $GdCrO_4$ at different temperatures between 4.2 and 36 K. The ratio of the two subspectra turns out to be 80–20%.

takes a value of $m_z = 1.0(2)\ \mu_B$, while the two components of the Gd^{3+} ordered moment are $m_z = 6.2(3)\ \mu_B$ and $m_x = 2.8(6)\ \mu_B$. Consequently, the modulus of the magnetic moment of the Gd^{3+} ion turns out to be $|m| = 6.8\ \mu_B$. Such a value is close to the theoretical one for the Gd^{3+} ion ($gJ = 7\ \mu_B$), so that it has almost reached saturation at a temperature of 2 K. Furthermore, it forms an angle of ≈24° with the *c*-axis. The obtained reliability factor of the refinement for the described magnetic structure is $R_{\mathrm{mag}} = 7.23$. Due to the tetragonal symmetry of the crystal structure, the orientation of the basal component of the ordered magnetic moments of the Gd^{3+} ions cannot be unequivocally determined in the *ab*-plane. This non-collinear ferromagnetic structure of $GdCrO_4$ does not evidence any significant change when the temperature is increased from 2 to 10 K, with the exception of a reduction of the ordered moments of both sublattices. Their experimental values at 10 K are: $m_z = 0.8(2)\ \mu_B$ (Cr^{5+}), $m_z = 4.9(3)\ \mu_B$ and $m_x = 2.5(6)\ \mu_B$ (Gd^{3+}), respectively.

3.5. ^{155}*Gd Mössbauer spectroscopy*

Figure 6 displays the recorded ^{155}Gd Mössbauer spectra of $GdCrO_4$ at different temperatures between 4.2 and 36 K. Astoundingly, the presence of two subspectra can be clearly observed in the temperature range mentioned. Its temperature-independent ratio turns out to be 80–20%. It is also surprising that at the value previously determined for its Curie temperature (22 K), only the 20% Gd site shows a magnetic order, while the remaining 80% Gd stays paramagnetic

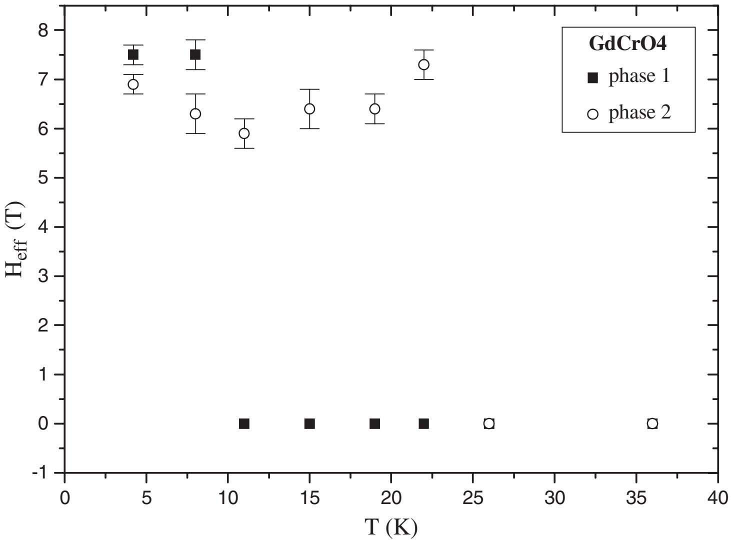

Figure 7. Temperature dependence of the hyperfine magnetic field of both the orthorhombic (1) and the tetragonal (2) phases present in $GdCrO_4$ between 4.2 and 36 K.

down to a temperature of 8 K. Based on the zircon-type structure and the previously described neutron diffraction results, only one subspectrum would be expected for $GdCrO_4$, since all Gd^{3+} ions occupy equivalent crystallographic positions. However, our recent ^{169}Tm Mössbauer spectroscopy results for the isostructural $TmCrO_4$ reveal the existence of two Tm sites, again with a proportion of 80–20%. In this oxide, an orthorhombic distortion has been observed by neutron diffraction experiments [26, 27]. Furthermore, similar structural distortions seem to be common in the $RCrO_4$ family of compounds, since a low-temperature orthorhombic symmetry has already been reported for $DyCrO_4$ [22] and $TbCrO_4$ [28]. Therefore, an orthorhombic distortion can also be suggested for $GdCrO_4$. In this sense, the 80% Gd site would correspond to the low-temperature orthorhombic phase, while the 20% Gd site could be ascribed to a remanent tetragonal phase. These results would also indicate that the instrumental resolution of the 7C2 diffractometer is not sufficient to detect the expected orthorhombic distortion in $GdCrO_4$.

The experimental value of the isomer shift at 4.2 K, relative to a source comprising Eu in Pd, is 0.63(1) mm s^{-1} for both subspectra. This value lies close to the one corresponding to $GdPO_4$ and $GdVO_4$ with respect to the same source, and fits well in the range of trivalent gadolinium [29]. The electric quadrupolar splittings of the two subspectra do not vary with temperature, and the absolute value of the main component of the electric field gradient ($|V_{zz}|$) is 32(3) V $Å^{-2}$ for the 80% subspectrum (phase 1) and 122(7) V $Å^{-2}$ for the 20% subspectrum (phase 2), respectively. Since the distortion may be relatively small, the expected asymmetry in the 80% subspectra has not been experimentally observed. Anyway, V_{zz} lies parallel to the c-axis for both crystal symmetries. Figure 7 shows the temperature dependence of the hyperfine magnetic field present in both subspectra. Whereas the hyperfine field of the 20% Gd site of 6.5(5) T remains relatively constant below 22 K, the one corresponding to the 80% site takes a value of 7.5(5) T only at temperatures lower than about 10 K, and it becomes zero at higher temperatures. Since the ^{155}Gd Mössbauer spectra of the two phases seem to be symmetric in the magnetically ordered state, it is not possible to determine the angle (θ) between V_{zz} and the hyperfine magnetic field. However, the determination of the magnetic structure of $GdCrO_4$

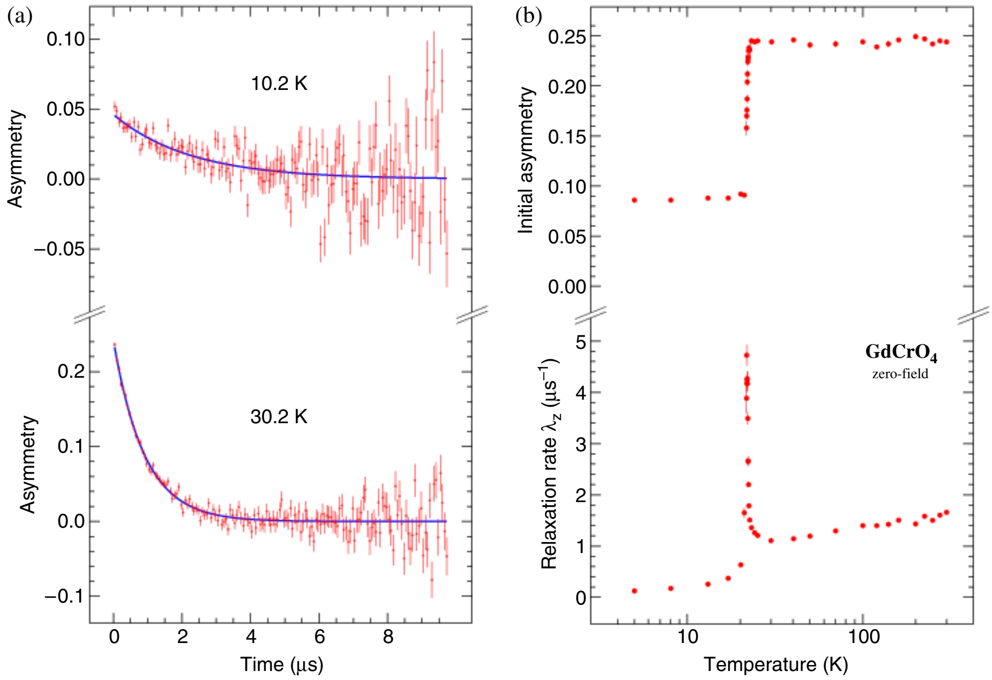

Figure 8. (a) μSR spectra of GdCrO$_4$ measured at $T = 10.2$ and 30.2 K. (b) Variation of both the initial asymmetry (a_0) and the relaxation rate (λ_z) with temperature. The magnetic ordering temperature obtained from these μSR experiments is 22.6 K.

by neutron diffraction experiments (see previous section) indicates that such an angle would take a value of $\theta \approx 24°$ for both phases. The magnetic hyperfine field in gadolinium nuclei is mainly determined by the Fermi contact interaction, which originates from the polarization of the core s electrons by the magnetic 4f electrons of the same atom. This polarization is commonly assumed to be constant, $B_C \approx -33.2$ T (the free ion value) [30]. Since GdCrO$_4$ possesses an insulator character, an additional polarization due to the 6s and 5d electrons of the same and/or neighbouring gadolinium atoms can be neglected. The experimental values of the hyperfine field of both subspectra are strongly reduced with respect to the mentioned free ion value. This significant reduction can only be attributed to the presence of a large transferred hyperfine field coming from the Cr^{5+} sublattice. In this case, the contributions of the Fermi contact interaction and the Gd–Cr transferred field would be opposed to one another, so as to yield a reduced effective hyperfine field.

3.6. μSR results

Zero-field μSR experiments have been performed on the powdered GdCrO$_4$ sample both in the ordered and paramagnetic states up to room temperature. Figure 8(a) collects the experimental data obtained at 10.2 and 30.2 K. Clear oscillations were not observed at any measuring temperature, even below its Curie temperature of 22 K. The data analysis has been carried out by using an exponential depolarization function:

$$a_0 P_z(t) = a_0 \exp(-\lambda_z t) \tag{2}$$

where a_0 and λ_z account for the initial asymmetry and the muon relaxation rate, respectively. Figure 8(b) displays the variation of both parameters with temperature between 5 and 300 K.

At a temperature of 22 K, the relaxation rate rapidly increases, attaining a maximum at 22.6(1) K. This fact, coupled with the loss of two-thirds of the initial asymmetry in this powdered sample, is characteristic of the magnetic ordering temperature. Such a value for the magnetic ordering temperature is in accordance with the one previously determined by bulk magnetic measurements, neutron diffraction and ^{155}Gd Mössbauer experiments. The magnetic phase transition takes place in just half a degree. Since only 20% of the Gd sublattice shows magnetic ordering at 22 K, we can conclude from the μSR results that the whole Cr^{5+} sublattice becomes magnetically ordered at the mentioned value of the Curie temperature in both phases. Furthermore, there is no sign of the second magnetic transition at around 10 K due to the 80% Gd ordering, which contradicts the ^{155}Gd Mössbauer results (see previous section). This discrepancy may be ascribed to the relatively low asymmetry present at low temperatures in this powder sample. A second fact to consider is the lack of information about the muon site in this compound. Since the muon chiefly probes the local magnetic field at its site, it may be that such a local field is not sensitive enough for the magnetic order in the Gd^{3+} sublattice, and only detects changes in the magnetic Cr^{5+} sublattice. Another important result to outline is the significant increase of the relaxation rate with temperature in the paramagnetic state. This effect constitutes a clear indication of the presence of short-range magnetic correlations above the Curie temperature [31, 32].

In order to pinpoint the effect of the Cr^{5+} ion on the overall magnetic properties of $GdCrO_4$, we have also measured $YCrO_4$ by the muon technique. The most salient feature of the μSR results for $YCrO_4$ is the lack of any temperature dependence of the relaxation rate in the paramagnetic regime within the experimental uncertainty, so that the Cr–Cr magnetic correlations are not intense enough to be detected by this technique. Therefore, the short-range magnetic correlations previously observed in $GdCrO_4$ can be mostly ascribed to the Gd–Cr magnetic interactions.

4. Conclusions

Study of the crystal structure of $GdCrO_4$ has been performed by room-temperature x-ray diffraction data. The derived structural parameters have been employed as initial values in the refinement of the neutron diffraction data between 2 and 300 K. In this way, accurate oxygen coordinates have been obtained which, in turn, have yielded appropriate bond distances and angles for the coordination polyhedron of both Cr^{5+} and Gd^{3+} ions. Furthermore, bulk magnetic measurements indicated the presence of a ferromagnetic order in this compound below $T_C = 22$ K. The analysis of the neutron diffraction pattern at lower temperatures has allowed us to determine the established magnetic structure. The ordered magnetic moment of the Cr^{5+} ion is located along the crystallographic *c*-axis, while that associated with the Gd^{3+} ion forms an angle of $\approx 24°$ with the mentioned axis.

Moreover, the specific heat measurements reveal the presence of a second weaker magnetic transition at lower temperatures. Such a transition has been confirmed by subsequent ^{155}Gd Mössbauer spectroscopy experiments. The Mössbauer spectra indicate that only 20% of Gd order magnetically at 22 K, while the remaining 80% do not show any magnetic order down to around 10 K. This 80% Gd site may be attributed to a low-temperature orthorhombic phase. The following μSR results indicate that the whole Cr^{5+} sublattice presents a magnetic order at the mentioned value of the Curie temperature. Besides that, short-range Gd–Cr magnetic correlations have been clearly observed in the paramagnetic state. Bearing all these facts in mind, we can conclude that the Cr^{5+} ion presents a ferromagnetic order at the temperature of 22 K, and induces the magnetic order in the 20% Gd^{3+} sublattice via a relatively large Gd–Cr exchange field. Since the ordered moments of both sublattices are not fully collinear (as expected due to the isotropic nature of the Gd^{3+} ion), a small anisotropic contribution should be present in the Gd–Cr magnetic exchange interactions. The magnetic order of the remaining 80% Gd^{3+} sublattice, resulting from an orthorhombic distortion, takes place at a lower temperature of around 10 K. However, further experimental evidence seems to be necessary to shed more light on the nature of this second magnetic transition. In this sense, the future availability of single crystals of this compound would be of great help, especially to further benefit from the μSR technique. The experimental observation of the magnetic order in the rare earth sublattice being induced by the Cr^{5+} order will help us to better understand the magnetic properties in the remaining $RCrO_4$ compounds during our ongoing research.

References

[1] Schwarz V H 1963 *Z. Anorg. Allg. Chem.* **323** 44
[2] Buisson G, Bertaut F and Mareschal J 1964 *C. R. Acad. Sci. Paris* **259** 411
[3] Greenblatt M, Pifer J H, McGarvey B R and Wanklyn B M 1981 *J. Chem. Phys.* **74** 6014
[4] Taylor K N R and Darby M I 1972 *Physics of Rare Earth Solids* (London: Chapman and Hall)
[5] Walter H, Kahle H G, Mulder K, Schopper H C and Schwarz H 1973 *Int. J. Magn.* **5** 129
[6] Stewart G A and Gubbens P C M 1999 *J. Magn. Magn. Mater.* **206** 17
[7] Jiménez E, Torralvo M J, Isasi J and Sáez-Puche R 2003 *Chem. Educador* **8** 60
[8] http://www-llb.cea.fr/spectros/spectros_e.html
[9] Wilson A J C (ed) *International Tables for Crystallography* vol C (Dordrecht: Kluwer–Academic)
[10] Young R A 1995 *The Rietveld Method* (Oxford: Oxford University Press)
[11] Rodríguez-Carvajal J 1993 *Physica* B **192** 55
For a more recent version see Rodríguez-Carvajal J 2001 recent developments of the Program FULLPROF *CPD Newslett.* **26** 12, available at http://journals.iucr.org/iucr-top/comm/cpd/Newsletters. The program can be obtained from the ftp-site: ftp://ftp.cea.fr/pub/llb/divers/fullprof.2k
[12] Mulay L N and Boudreaux E 1976 *Theory of Molecular Paramagnetism* (New York: Wiley) p 494
[13] Bachman R *et al* 1972 *Rev. Sci. Instrum.* **43** 205
[14] Stewart G A 1994 *Mater. Forum* **18** 177
[15] Dirken M W, Thiel R C, Coehoorn R, Jacobs T H and Bushow K H J 1989 *J. Less-Common Met.* **155** 339
[16] Dalmas de Réotier P and Yaouanc A 1997 *J. Phys.: Condens. Matter* **9** 9113
[17] Karlsson E B 1995 *Solid State Phenomena as Seen by Muons, Protons and Excited Nuclei* (Oxford: Clarendon)
[18] http://lmu.web.psi.ch/facilities/gpd/gpd.html
[19] Jiménez E, Isasi J and Sáez-Puche R 2002 *J. Solid State Chem.* **164** 313
[20] Jiménez E, Isasi J and Sáez-Puche R 2000 *J. Alloys Compounds* **312** 53
[21] Nyman H, Hyde B G and Anderson S 1984 *Acta Crystallogr.* B **40** 441
[22] Tezuka K and Hinatsu Y 2001 *J. Solid State Chem.* **160** 362
[23] Gopal E S R 1966 *Specific Heats at Low Temperatures* (New York: Plenum)
[24] Metcalfe M J and Rosenberg H M 1970 *Phys. Lett.* A **33** 211
[25] Metcalfe M J and Rosenberg H M 1972 *J. Phys. C: Solid State Phys.* **5** 459
[26] Jiménez E, Gubbens P C M, Sakarya S, Stewart G A, Dalmas de Réotier P, Yaouanc A, Isasi J, Sáez-Puche R and Zimmermann U 2004 *J. Magn. Magn. Mater.* **272–276** 568
[27] Sáez-Puche R, Jiménez E, Isasi J, Fernández-Díaz M T and García-Muñoz J L 2003 *J. Solid State Chem.* **171** 161
[28] Buisson G, Cheou T, Sayetat F and Scheunemann K 1976 *Solid State Commun.* **18** 871
[29] Cashion J D, Prowse D B and Vas A 1973 *J. Phys. C: Solid State Phys.* **6** 2611
[30] Baker J M and Williams F I B 1962 *Proc. R. Soc.* A **267** 283
[31] Hartmann O, Karlsson E, Wappling R, Chappert J, Yaouanc A, Ash L and Kalvius G M 1986 *J. Phys. F: Met. Phys.* **16** 1593
[32] Dalmas de Réotier P, Yaouanc A, Gubbens P C M, Sakarya S, Jiménez E, Bonville P and Hodges J A 2004 *Hyperfine Interact.* **158** 131